European Journal of Medicinal Chemistry 245 (2023) 114927

Contents lists available at ScienceDirect

European Journal of Medicinal Chemistry

journal homepage: www.elsevier.com/locate/ejmech

Research paper

Discovery of PPARγ and glucocorticoid receptor dual agonists to promote the adiponectin and leptin biosynthesis in human bone marrow mesenchymal stem cells

Sungjin Ahn [a], Myunghwan Ahn [b], Suzie Park [b], Seungchan An [a], In Guk Park [a], Seok Young Hwang [a], Junpyo Gong [a], Soyeon Oh [a], Sun Hee Jin [a], Hee Jin Kim [c], Jae Hoon Cheong [d], Youngjoo Byun [b,*], Minsoo Noh [a,**]

[a] College of Pharmacy, Natural Products Research Institute, Seoul National University, Seoul, 08826, Republic of Korea
[b] College of Pharmacy, Korea University, 2511 Sejong-ro, Sejong, 30019, Republic of Korea
[c] Uimyung Research Institute for Neuroscience, Sahmyook University, 26-21 Kongreung-2-dong, Hwarangro-815, Nowon-gu, Seoul, 139-742, Republic of Korea
[d] School of Pharmacy, Jeonbuk National University, Jeonju, 54896, Republic of Korea

ARTICLE INFO

Keywords:
Adiponectin
Leptin
Human bone marrow mesenchymal stem cells
Target identification
PPARγ and glucocorticoid receptor dual modulator

ABSTRACT

Adiponectin and leptin are major adipocytokines that control crosstalk between adipose tissue and other organ systems. Hypoadiponectinemia and hypoleptinemia are associated with human metabolic diseases. Compounds with adipocytokine biosynthesis-stimulating activities could be developed as therapeutics against diverse metabolic conditions. In phenotypic screening with human bone marrow mesenchymal stem cells (hBM-MSCs), (*E*)-4-hydroxy-3-(3-(4-hydroxy-3-methoxyphenyl)acryloyl)-6-methyl-2*H*-pyran-2-one (**1**) was identified to increase adiponectin biosynthesis during adipogenesis and simultaneously to stimulate leptin production. Using the compound **1** structure, the structure-activity relationship study was performed to discover more potent compounds stimulating both adiponectin and leptin production. (*E*)-3-(3-(2-fluoropyridin-4-yl)acryloyl)-4-hydroxy-6-methyl-2*H*-pyran-2-one (**11**) exhibited the most potent adiponectin (EC_{50}, 2.87 μM) and leptin (EC_{50}, 2.82 μM) biosynthesis-stimulating activities in hBM-MSCs. In a target identification study, compound **11** was characterized as a dual modulator binding to both peroxisome proliferator-activated receptor (PPAR) γ and glucocorticoid receptor (GR). This study provides a novel pharmacophore for PPARγ/GR dual modulators with therapeutic potential against human metabolic diseases.

1. Introduction

Adipocytes in normal fat tissues produce diverse adipocytokines that can regulate metabolic crosstalk between fat and other tissues, including the muscle, liver, and brain [1]. Adipocytokines with autocrine, paracrine, and hormonal functions play critical roles in regulating systemic metabolic homeostasis. Adiponectin affects the regulation of lipid metabolism, insulin sensitivity and, inflammatory processes [2]. Leptin acts centrally on the hypothalamus to regulate food consumption and energy balance. In addition to its central role, leptin exerts a regulatory role in peripheral tissues. For example, leptin directly promotes fatty acid oxidation in adipose tissues and the liver [3]. Genetic polymorphisms or defects in both adiponectin and adiponectin receptor have been associated with various metabolic diseases [4]. In patients with lipodystrophy, deficiency of adiponectin and leptin can cause severe insulin resistance and metabolic complications [5]. Relative hypoleptinemia has also been reported in type I and type II diabetic patients [6]. In this regard, compounds capable of stimulating adiponectin and/or leptin production in adipocytes have been suggested as novel therapeutics for diverse metabolic diseases [7].

To discover adipocytokine biosynthesis-stimulating compounds, phenotype-based approaches can be designed using the adipogenesis model of human bone marrow mesenchymal stem cells (hBM-MSCs) [8–10]. Adiponectin biosynthesis-stimulating compounds can be identified during adipogenesis in hBM-MSCs by co-treatment with an adipogenesis-inducing chemical cocktail consisting of insulin,

* Corresponding author.
** Corresponding author.
E-mail addresses: yjbyun1@korea.ac.kr (Y. Byun), minsoonoh@snu.ac.kr (M. Noh).

https://doi.org/10.1016/j.ejmech.2022.114927
Received 27 August 2022; Received in revised form 9 November 2022; Accepted 9 November 2022
Available online 10 November 2022

dexamethasone and 3-isobutyl-1-methylxanthine (IDX condition). Compounds capable of stimulating leptin production can be screened by employing differentiated adipocytes derived from hBM-MSCs. Interestingly, hBM-MSCs produce leptin in response to glucocorticoids such as dexamethasone [11]. Phenotypic screening of hBM-MSCs revealed that (*E*)-4-hydroxy-3-(3-(4-hydroxy-3-methoxyphenyl)acryloyl)-6-methyl-2*H*-pyran-2-one (**1**), a natural compound isolated from *Pogostemon heyneanus*, increased adiponectin production during adipogenesis in hBM-MSCs, as well as stimulated leptin production in hBM-MSCs. In the present study, we aimed to synthesize more potent compounds with adiponectin and leptin production-stimulating activities based on the chemical structure of compound **1** for target identification.

2. Results and discussion

2.1. Synthesis of compound 1 derived from the P. heyneanus and its analogs

Scheme 1 describes the synthesis of compound **1** and its analogs, with variations in the vanillin region. We performed aldol condensation of dehydroacetic acid with the appropriate aldehyde in the presence of piperidine in chloroform under reflux, which afforded compounds **1**–**16** in moderate to high yields. The (*E*) geometrical isomer was obtained in the major form and was confirmed based on the integration and coupling constant (>15 Hz) of the chalcone group from the ^{1}H NMR experiment. The purity of compounds **1**–**16** was confirmed by high-pressure liquid chromatography (HPLC) with two different solvent systems (acetonitrile/water and methanol/water; Supplementary Figs. S17–S48).

2.2. Validation of adipocytokine biosynthesis-stimulating activity of the synthetic compound 1 in hBM-MSCs

To evaluate the adipocytokine biosynthesis-stimulating activities of *P. heyneanus* derived (*E*)-4-hydroxy-3-(3-(4-hydroxy-3-methoxyphenyl) acryloyl)-6-methyl-2*H*-pyran-2-one (GPL3A04) and its synthetic compound **1**, hBM-MSCs-based phenotype assay was performed. The naturally isolated compound **1** and its synthetic compound **1** significantly promoted adiponectin production by 3.30- and 3.18-fold at 30 μM when compared with the IDX control, respectively (Fig. 1A). On measuring lipid accumulations levels of differentiated hBM-MSCs using Oil Red O staining, compound **1** increased the number of lipid droplets when compared with that of the IDX control (Fig. 1B). Positive controls, pioglitazone and glibenclamide, also increased lipid droplet formation during adipogenesis in hBM-MSCs, as reported in the literature [12–14]. However, the effects of compound **1** were less potent than those of glibenclamide and pioglitazone. To compare the leptin biosynthesis-stimulating activities of naturally isolated compound **1** and synthetic compound **1**, hBM-MSCs were treated with the respective compounds, and leptin secretion was quantified using ELISA (Fig. 1C). Synthetic compound **1** significantly increased leptin biosynthesis by 2.58-fold at 30 μM when compared with Dulbecco's Modified Eagle Medium (DMEM) control and was as potent as that of the naturally isolated compound **1** (Fig. 1D). Therefore, the adipocytokine biosynthesis-stimulating activity of naturally isolated compound **1** in the chemical library was validated using its synthetic compound **1**.

2.3. Chemistry for the structure-activity relationship study

Compound **1** exhibited significant adipocytokine biosynthesis-stimulating activity for both adiponectin and leptin, however, its

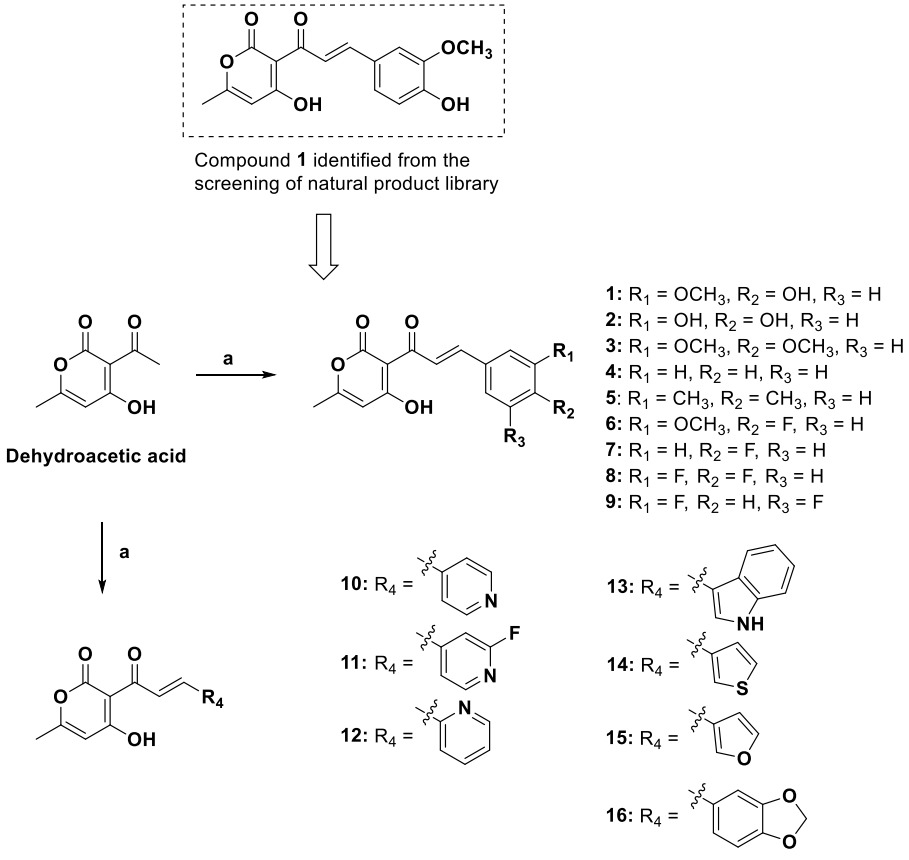

Scheme 1. Synthetic route for the synthesis of chalcone analogs. Reagents and conditions: (a) appropriate aldehyde (1 equiv), piperidine (0.8 equiv), $CHCl_3$, reflux, 6–16 h.

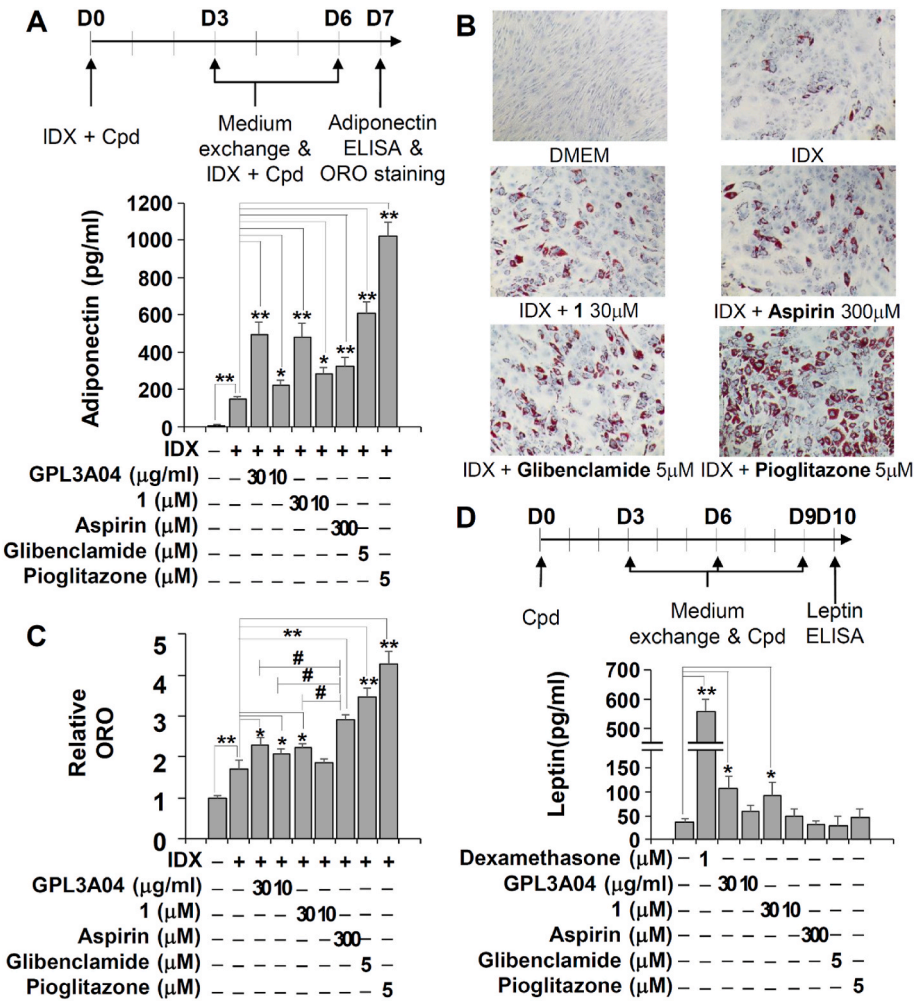

Fig. 1. Validation of the adipocytokine biosynthesis-stimulating activity of *Pogostemon heyneanus*-derived compound **1** (code: GPL3A04) with its synthetic analog compound **1**. (A) To evaluate adiponectin production-stimulating activity of GPL3A04 and its synthetic analog compound **1**, compounds were co-treated with the adipogenesis-inducing chemical cocktail (IDX) medium in hBM-MSCs. The IDX medium with compounds was changed on the third and sixth day. On the seventh day, the cell culture supernatants were collected and the level of adiponectin was evaluated using an enzyme-linked immunosorbent assay (ELISA). Aspirin, glibenclamide, and pioglitazone were used as positive controls. (B) To detect the lipid droplet induction within cultured cells, Oil Red O (ORO) and hematoxylin staining were performed on the seventh day. (C) Relative ORO staining quantification was measured at 540 nm. (D) To quantify leptin production-stimulating activity of GPL3A04 and its synthetic analog compound **1**, compounds were treated with high glucose DMEM medium in hBM-MSCs. The DMEM medium with compounds was exchanged on the third, sixth, and ninth days. On the tenth day, the cell culture supernatants were collected and the level of leptin was evaluated using ELISA. Dexamethasone was used as a positive control. Values represent the means ± SD ($n = 3$); $^{*}p \leq 0.05$, $^{\#}p \leq 0.05$ and $^{**}p \leq 0.01$.

effect on leptin was insufficient for use in subsequent target identification studies. Thus, new compounds were synthesized to find compound **1** derivatives with potent adipocytokine biosynthesis-stimulating activity. Compound **1** contained 2H-pyran-2-one, chalcone and 4-hydroxy-3-methoxyphenyl moieties. We focused on the structural modification of the substituted phenyl moiety while leaving the 2H-pyran-2-one and chalcone regions intact. The substituents (4-OH and 3-OCH_3) of compound **1** were replaced with –H, –F, –OH, $–CH_3$, and $–OCH_3$ to determine the effect of substituents on the adipocytokine biosynthesis-stimulating activity. The phenyl ring was replaced by a heteroaromatic ring (e.g, pyridine, indole, furan, thiophene).

2.4. Adipocytokine biosynthesis-stimulating activities of novel compound *1* derivatives

The adipocytokine biosynthesis-stimulating activities of novel synthetic derivatives were evaluated in hBM-MSCs. Compared with the IDX control, compounds **1**–**16**, except **9**, significantly increased adiponectin production, as determined in the adipocyte differentiation model of hBM-MSCs (Table 1). In the leptin biosynthesis-stimulating activity assay in hBM-MSCs, compounds **1**, **3**, **8**, **10**, **11**, **12**, **14**, **15**, and **16** significantly stimulated leptin production when compared with the medium control; however, **2**, **4**, **5**, **6**, **7**, **9**, and **13** did not alter leptin biosynthesis. Considering the structure-activity relationship with adipocytokine biosynthesis-stimulating activity, the conversion of phenyl residue to pyridine or 2-fluoropyridine afforded robust adipocytokine biosynthesis-stimulating activity. In addition, when the phenyl group of compound **1** was substituted with heteroaryl moieties such as thiophene or furan, the leptin production-stimulating activity was increased. Among the adipocytokine biosynthesis-stimulating compounds, compounds **10** and **11** were selected for subsequent concentration-effect analysis, given their potent stimulatory effects on adipocytokine biosynthesis. For the concentration-effect analysis of adiponectin production, the half-maximal effective concentration (EC_{50}) values were calculated by setting the maximal effect of pioglitazone, a currently prescribed PPARγ agonist, to 100%. The EC_{50} values of compounds **10** and **11** were 9.3 and 2.9 μM, respectively, which were less potent than pioglitazone (EC_{50} 0.6 μM) (Fig. 2A). The EC_{50} values were calculated based on the maximum effect of dexamethasone as 100% for the concentration-effect analysis of leptin production. The EC_{50} values for compounds **10** and **11** were 8.5 and 2.2 μM, respectively (Fig. 2B).

2.5. Target identification of adipocytokine biosynthesis-stimulating compounds *10* and *11*

Transcription-regulating nuclear receptors such as PPARα, PPARγ, PPARδ, farnesoid X receptor (FXR) and GR are associated with the cellular regulation of the adipocytokine biosynthesis in mammalian adipocytes [15–17]. Radioligand-binding assays were performed on nuclear receptors to identify molecular targets of compounds **10** and **11** mediating the adiponectin and leptin biosynthesis-stimulating activities. In the radioligand-binding assay, compounds **10** and **11** competitively bound to PPARγ and GR, however, did not replace the labeled ligand competitive binding to PPARα and PPARδ (Fig. 3A). In a

Table 1

Adipocytokine biosynthesis-stimulating activities of novel compound 1 derivatives[a].

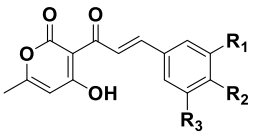

1-9

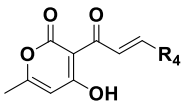

10-16

Cpd	R_1	R_2	R_3	R_4	Adiponectin (pg/ml) at 10 μM[b]	Leptin (pg/ml) at 10 μM[c]
1	OCH_3	OH	H		399 ± 60**	82 ± 40*
2	OH	OH	H		243 ± 48*	16 ± 3
3	OCH_3	OCH_3	H		747 ± 34**	80 ± 48*
4	H	H	H		580 ± 106**	38 ± 30
5	CH_3	CH_3	H		438 ± 71**	17 ± 57
6	OCH_3	F	H		567 ± 91**	40 ± 27
7	H	F	H		576 ± 76**	30 ± 59
8	F	F	H		432 ± 68**	76 ± 21*
9	F	H	F		172 ± 56	33 ± 48
10				pyridin-4-yl	839 ± 66**	496 ± 50**
11				2-fluoropyridin-4-yl	769 ± 64**	587 ± 15**
12				pyridin-2-yl	396 ± 67**	95 ± 18*
13				1H-indol-3-yl	396 ± 68**	41 ± 36
14				thiophen-3-yl	486 ± 86**	193 ± 56**
15				furan-3-yl	320 ± 59**	171 ± 33**
16				benzo[d] [1,3]dioxol-5-yl	208 ± 87*	91 ± 15*
DMEM cont						18 ± 18
IDX cont					100 ± 57	
Aspirin (300 μM)					330 ± 15**	20 ± 17
Glibenclamide (5 μM)					475 ± 21**	30 ± 35
Pioglitazone (5 μM)					812 ± 49**	33 ± 16
Dexamethasone (1 μM)						632 ± 43**

[a] Values represent the means ± SD ($n = 3$, three independent experiments); *$p \leq 0.05$ and **$p \leq 0.01$.

[b] In the adipogenic differentiation model of hBM-MSCs, cell culture supernatants were harvested and adiponectin biosynthesis-stimulating activity was measured by ELISA.

[c] The leptin biosynthesis-stimulating activity of compound **1** and its derivatives was evaluated using hBM-MSCs cultured in DMEM.

concentration-response assessment of GR binding, the *Ki* value of **11** was 33.6 μM, which was not as potent as dexamethasone (*Ki* value 2.9 nM). Although **10** significantly bound to GR when compared with vehicle control, the *Ki* value was not derived, as it replaced only 43.3% at 30 μM (Fig. 3B). In a concentration-response analysis of PPARγ binding, *Ki* values for compounds **10** and **11** were 12.9 and 3.3 μM, respectively (Fig. 3C). In addition, previous studies have reported that inhibition of PPARγ phosphorylation by cyclin-dependent kinase 5 (CDK5) could modulate adipocytokine biosynthesis [18,19]. On examining the effect of compounds **10** and **11** on CDK5 activity, neither compound exerted any effect on CDK5 activity at concentrations up to 30 μM (Fig. 3D). Therefore, the adipocytokine biosynthetic activity of compounds **10** and **11** in hBM-MSCs was attributed to the dual modulation of PPARγ and GR.

2.6. Polypharmacological evaluation of compounds *10* and *11*

Next, to determine the polypharmacological profile of compounds **10** and **11** for PPARγ and GR, full agonists or antagonists were co-administered with compounds **10** or **11** in hBM-MSCs (Fig. 4). First, to validate whether compounds **10** and **11** are full or partial PPARγ agonists, both compounds were co-treated with pioglitazone, a full agonist of PPARγ, or T0070907, an antagonist of PPARγ in hBM-MSCs. Similarly, compounds **10** and **11** also stimulated adiponectin production in a concentration-dependent manner when treated alone, and the adiponectin-promoting effect was antagonized when treated with T0070907. This indicates that the adiponectin biosynthesis-stimulating effects of compounds **10** and **11** are dependent on the PPARγ agonistic effect. Co-treatment with compound **10** and 1 μM pioglitazone exhibited additive adiponectin biosynthesis-stimulating effects, suggesting that compounds **10** functioned as a PPARγ full agonist (Fig. 4A). Compound **11** was also determined as a PPARγ full agonist (Fig. 4B). Next, compounds **10** and **11** were co-treated with the GR agonist, dexamethasone, a GR full agonist, or mifepristone, a GR antagonist in hBM-MSCs. Dexamethasone increased leptin levels in a concentration-dependent manner, whereas 1 μM the mifepristone antagonized the dexamethasone-induced leptin biosynthesis. Furthermore, following co-treatment with dexamethasone, compound **10** exhibited an additive leptin biosynthesis effect in hBM-MSCs and mifepristone antagonized the leptin biosynthesis induced by compound **10** (Fig. 4C). Similar results were obtained when compound **11** was examined under the identical conditions (Fig. 4D). These results indicated that compounds **10** and **11** functioned as GR full agonists. Taken together, compounds **10** and **11** have pharmacophores of PPARγ and GR dual agonists.

2.7. Molecular modeling of GR and PPARγ with compound *11*

In radioligand-binding assays, compound **11** directly interacted with PPARγ and GR. To elucidate the binding mode of compound **11**, molecular modeling studies of compound **11** with PPARγ and GR were performed using the GR and PPARγ protein crystal structures in the RCSB Protein Data Bank (PDB) (Fig. 5). First, molecular interaction models of compound **11** or pioglitazone within the ligand-binding domain (LBD) of PPARγ were analyzed using the PDB PPARγ structure 2PRG [20]. Pioglitazone, a PPARγ full agonist, formed a C-shaped arrangement centered on helix 3 in the PPARγ LBD and formed hydrogen bonds with Gln 286, His 323, and Tyr 473 (Fig. 5A). Ligand interactions with Tyr 473 stabilize the H12 of the PPARγ LBD, which is essential for recruiting diverse coactivator proteins that regulate the transcription of PPARγ target genes [21]. In addition, Met 346 formed a pi-sulfur interaction and Cys 285, Arg 288, Leu 330, and Ile 341 established pi-alkyl interactions with pioglitazone within the PPARγ-LBD (Fig. 5A). Similar to pioglitazone, the energy-minimized model revealed that compound **11** formed a C-shaped arrangement around H3 (Fig. 5B). Amino acid residues, Cys 285, Gln 286, Ser 289, His 323, His 449, and Tyr 473 in PPARγ-LBD interacted with compound **11** via hydrogen

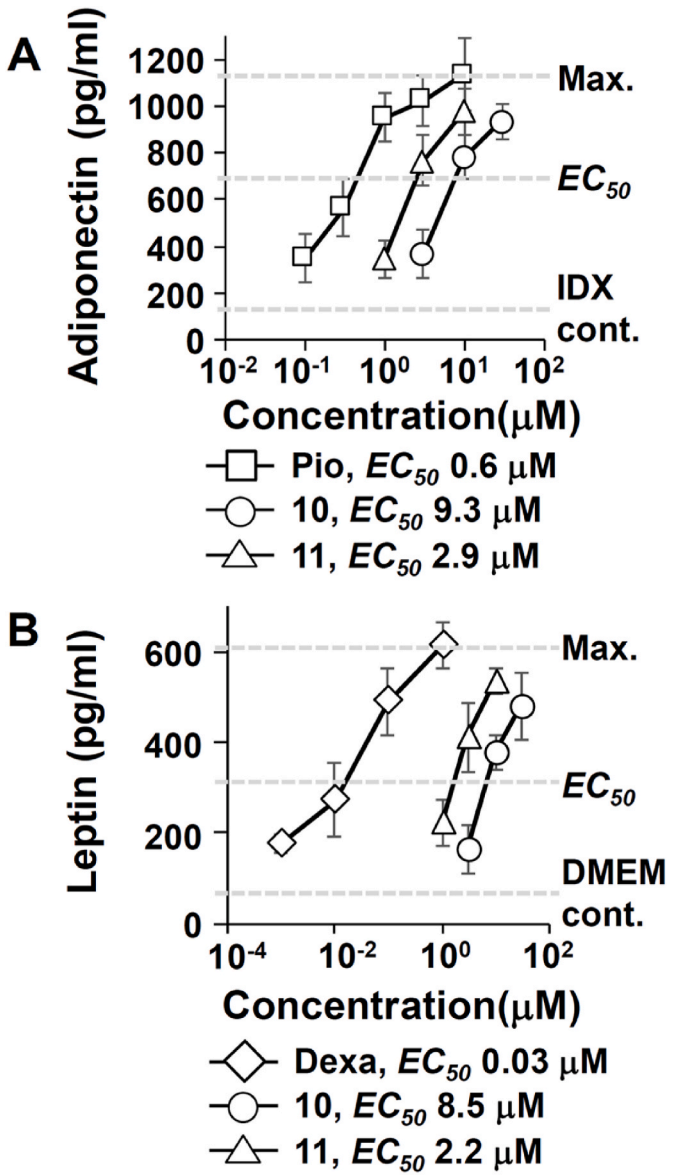

Fig. 2. The concentration-effect analysis of adipocytokine biosynthesis-stimulating compounds **10** and **11**. The EC_{50} values for compounds **10** and **11** were calculated in the concentration-dependent curve of adiponectin and leptin production-stimulating activities. (A) In the adipogenic differentiation model of hBM-MSCs, cell culture supernatants were harvested and adiponectin biosynthesis-stimulating activity was measured by ELISA. Pioglitazone (Pio) was used as a positive control. (B) The leptin biosynthesis-stimulating activity of compound **1** and its derivatives were evaluated using hBM-MSCs cultured in DMEM. Dexamethasone (Dexa) was used as a positive control. Values represent the means ± SD ($n = 3$).

bonds. In addition, compound **11**-bound PPARγ-LBD model exhibited hydrophobic interactions with Arg 288 and His 449 (Fig. 5B). Therefore, the optimized docking model supported that compound **11** functioned as a PPARγ full agonist, similar to pioglitazone.

Next, molecular interaction models of compound **11** or dexamethasone with GR-LBD were performed using the PDB GR protein structure 6EL9, consisting of 12 α and 4 β helices [22]. Typically, the agonist binding to GR-LBD stabilized the active conformation of the AF-2 domain of H3, H4, and H12 in GR, which is required to recruit various coactivator proteins such as SRC, and TIF-2 [23–25]. In the optimized docking model, dexamethasone interacted with GR-LDB via hydrogen bonds with Leu536, Asn 564, Gln 642 and Thr 739 and formed alkyl interactions with Met 601, Met 604, Leu 732, Tyr 735 and Cys 736. Ligand interactions with Tyr735 and Thr739 in GR-LBD are well-known features that distinguish between GR agonists and antagonists [26,27]. The interactions of agonists with both Tyr 735 and Thr 739 are essential for transactivating GR target genes. In contrast to GR agonists, GR antagonists such as mifepristone lacked molecular interactions with Tyr735 and Thr739 [26]. In the docking model, interactions with both Tyr735 and Thr739 existed in the dexamethasone-bound GR-LBD (Fig. 5C). The molecular docking model of compound **11** against GR-LBD exhibited the typical features of GR agonists, such as dexamethasone. In particular, the nitrogen atom on the pyridine-4-yl group of compound **11** contributed to the formation of hydrogen bonds with Gln 642. Since Gln 642 was known to play an important role in the binding of GR agonists in mutagenesis studies [28], it can be inferred that pyridine-4-yl derivatives **10** and **11** had stronger leptin biosynthesis-stimulating activity than other compounds. Compound **11** also formed not only hydrogen bonds with Gly 567, Met 646, and Thr 739 but also exhibited hydrophobic interactions with Met 604 and Tyr 735. In line with the experimental data, the molecular interaction model supported that compound **11** was a GR agonist.

*2.8. Anti-diabetic activity of compound **11** in a streptozotocin (STZ)-induced diabetic mouse model*

The adipocytokine biosynthesis-stimulating compound **11** has a polypharmacophore that binds to PPARγ and GR. Some patients with metabolic diseases experience hypoadiponectinemia and/or hypoleptinemia [29,30]. To further prove that adipocytokine biosynthesis-stimulating compound **11** has therapeutic potential in human metabolic diseases, the insulin-sensitizing activity of compound **11** in the STZ-induced mouse model was investigated (Fig. 6). The significant anti-diabetic activity was observed in the compound **11**–treated group on the second day of treatment in a dose-dependent manner when compared with that in the vehicle-treated group (Fig. 6A). In general, serum lactate levels are chronically increased in diabetic patients with obesity when compared with those in healthy individuals; therefore, hyperlactatemia is associated with the onset of insulin resistance [31]. On the 5th day of daily treatment, compound **11** significantly downregulated serum lactate levels in a dose-dependent manner when compared with the vehicle control (Fig. 6B). These results showed that compound **11** could potentially reduce the risk of metabolic acidosis related to diabetic complications or medication such as metformin. Furthermore, compound **11** significantly increased serum adiponectin levels when compared with the control (Fig. 6C). Therefore, dual PPARγ and GR modulator compound **11** exhibits therapeutic potential to improve adverse outcomes of human metabolic diseases.

2.9. Therapeutic potential of adipocytokine biosynthesis-stimulating PPARγ/GR dual modulators

Compounds **10** and **11** exhibit a novel polypharmacological profile, i.e., PPARγ and GR dual agonists, and they have adiponectin and leptin biosynthesis-stimulating activities. The use of small molecules to promote adiponectin biosynthesis could ameliorate diabetes, non-alcoholic steatohepatitis (NASH), cardiovascular disease, and cancers associated with glucose and lipid metabolism [32]. Exogenous leptin treatment was shown to improve hyperglycemia and hyperketonemia in animal models [33] and had beneficial effects on various metabolic diseases, such as lipodystrophy and NASH [34]. In addition, the co-regulation of GR and PPARγ has beneficial effects on maintaining lipid homeostasis, owing to the balanced control between lipolysis and lipogenesis in adipocytes [35]. In the present study, compound **11** improved diabetic lactic acidosis in the STZ-induced diabetic mouse model. As adipocytokine biosynthesis-stimulating compounds, i.e., PPARγ and GR dual modulators, compound **1** and its synthetic derivatives conclusively have therapeutic potentials in diverse metabolic diseases.

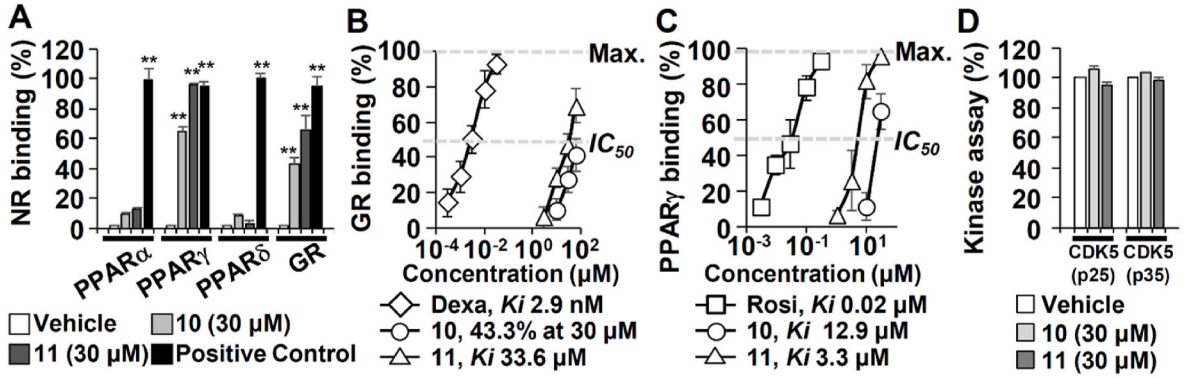

Fig. 3. The target identification of compounds **10** and **11**. (A) Competitive radioligand binding assays of nuclear receptor (PPARα, PPARγ, PPARδ, and GR) were performed for compounds **10** and **11**. The positive controls were WY-14643 for PPARα, rosiglitazone (Rosi) for PPARγ, L-783483 for PPARδ, and dexamethasone (Dexa) for GR. The concentration-dependent binding activities of compounds **10** and **11** were determined with radioligand binding assays for GR (B) and PPARγ (C). *Ki* values of compounds **10** and **11** were calculated by the Cheng and Prusoff equation. (D) The kinase activity was evaluated by measuring the γ-^{32}P-ATP incorporation to CDK complexes. The inhibitory activities of compounds **10** and **11** on the phosphorylation of CDK5/p25 and CDK5/p35 were tested at each K_m ATP concentration. DMSO was included in each negative control. Values represent the means ± SD ($n = 3$); $^*p \leq 0.05$ and $^{**}p \leq 0.01$.

Regarding to inflammation, PPARγ and GR dual modulators can induce additive or synergistic anti-inflammatory effects. Glucocorticoids are well-known anti-inflammatory compounds in general [36]. Recently, direct anti-inflammatory activity was reported in the study on the effects of PPARγ agonists on macrophage functions [37]. Co-modulation of PPARγ and GR resulted in the improvement of various inflammatory responses in animal models for atopic march and chronic gastric ulcer [38,39]. Notably, co-treatment of glucocorticoids and PPARγ agonists reportedly attenuates the major adverse effects of glucocorticoid treatment, such as skin barrier disruption, in animal models of dermatological diseases [40]. In addition, PPARγ ligands potentiated the therapeutic effect of glucocorticoids in nephrotic syndrome [41]. Accordingly, the therapeutic benefits of PPARγ and GR dual modulators should be further investigated in diverse disease models.

As PPARγ and GR dual modulators, compound **1** and its synthetic derivatives exhibit non-thiazolidinedione PPARγ functions and non-steroidal GR agonistic activities. Several thiazolidinedione class PPAR agonists have been withdrawn owing to their serious adverse effects on diverse physiological systems [42,43]. Numerous studies have reported the discovery of non-thiazolidinedione PPARγ specific agonists, dual modulators, or pan-modulators, with the expectation of less serious side effects [44–46]. Notably, serious side effects related to glucocorticoid therapy could be improved by using the non-steroidal GR agonist functions of compound **1** and its synthetic derivatives. From this toxicological perspective, compound **1** and its synthetic derivatives should be validated in future research.

3. Conclusions

Herein, a novel PPARγ and GR dual modulator was discovered from the structure activity relationship study of compound **1** derived from *P. heyneanus*. Compound **1** and its synthetic derivatives had adipocytokine biosynthesis-stimulating effects in hBM-MSCs. Among synthetic derivatives, compound **11** exhibited the most potent adiponectin and leptin biosynthesis-stimulating activities and following target identification elucidated its pharmacological mechanism as a PPARγ and GR dual modulator. Compound **11** improved hyperglycemic conditions and serum adiponectin profiles in the STZ-induced diabetic mice. Notably, compound **1** and its synthetic derivatives provide a novel pharmacophore for PPARγ and GR dual modulators with therapeutic potential for human metabolic diseases. To develop these PPARγ and GR dual modulators as novel therapeutics for human metabolic diseases, further studies will be needed in terms of efficacy and toxicity in the future.

4. Experimental section

4.1. General methods

All chemicals and solvents used in the reaction were purchased from Sigma−Aldrich, TCI, and Acros and were used without further purification. Reaction progress was monitored by TLC on pre-coated silica gel plates with silica gel 60F_{254} (Merck; Darmstadt, Germany) and visualized by UV254 light and/or $KMnO_4$ staining for detection purposes. Column chromatography was performed on silica gel (Silica gel 60; 230–400 mesh ASTM, Merck, Darmstadt, Germany). Nuclear magnetic resonance (NMR) spectra were recorded at room temperature on a BRUKER BioSpin AVANCE 300 MHz NMR (^{1}H, 300 MHz; ^{13}C, 75 MHz) or a Bruker UltraShield 600 MHz Plus (^{1}H, 600 MHz; ^{13}C, 150 MHz) spectrometer. All chemical shifts are reported in parts per million (ppm) from tetramethylsilane ($\delta = 0$) and were measured relative to the solvent in which the sample was analyzed ($CDCl_3$: δ 7.26 for ^{1}H NMR, δ 77.0 for ^{13}C NMR; DMSO−d_6: δ 2.50 for ^{1}H NMR, δ 39.52 for ^{13}C NMR). The ^{1}H NMR shift values are reported as chemical shift (δ), the corresponding integral, multiplicity (s = singlet, br = broad, d = doublet, t = triplet, q = quartet, m = multiplet, dd = doublet of doublets), coupling constant (J in Hz) and assignments. High resolution mass spectra (HRMS) were recorded on an Agilent 6530 Accurate Mass Q-TOF LC/MS spectrometer. Melting point of the final compounds was measured by hot stage microscopy using a Linkam THMS600 variable temperature stage (Linkam Instruments, Tadworth, U.K.) with a polarizing optical microscope, NIKON Eclipse LV100POL (NIKON, NY, USA) equipped with a Nikon DS-Fi1 camera and Nikon NIS-Elements BR software (ver. 4.00.06) and Linksys 32 software data capture system (Linkam Instruments, Tadworth, U.K). The purity of the final compounds was measured by analytical RP-HPLC on an Agilent 1260 Infinity (Agilent) with a C18 column (Phenomenex, 150 mm × 4.6 mm, 3 μm, 110 Å). RP-HPLC was performed on two different solvent systems using the following isocratic conditions: for method A, the mobile phase was ACN and water (50:50, *v/v*, 0.1% TFA); for method B, the mobile phase was ACN and water (40:60, *v/v*, 0.1% TFA); for method C, the mobile phase was ACN and water (30:70, *v/v*, 0.1% TFA); for method D, the mobile phase was ACN and water (15:85, *v/v*, 0.1% TFA); for method E, the mobile phase was MeOH and water (70:30, *v/v*, 0.1% FA); for method F, the mobile phase was MeOH and water (65:35, *v/v*, 0.1% FA); for method G, the mobile phase was MeOH and water (60:40, *v/v*, 0.1% FA); for method H, the mobile phase was MeOH and water (50:50, *v/v*, 0.1% FA); for method I, the mobile phase was MeOH and water (30:70, *v/v*, 0.1% FA). All compounds were eluted with a flow rate of 1.0 mL/min (method A to D) or 0.7 mL/min (method E to I) and monitored using a UV detector: 254

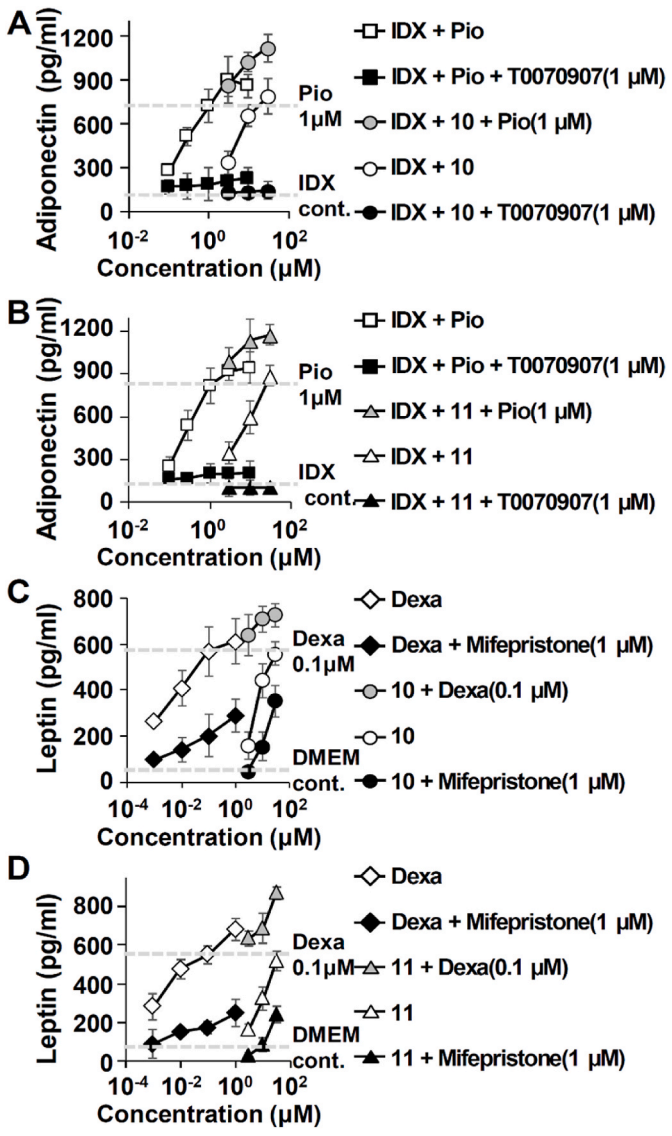

Fig. 4. Evaluation of the PPARγ full agonism and GR full agonism of compounds **10** and **11**. Adipocytokines production-stimulating activities were validated by co-treatment of compounds **10** or **11** in the presence of agonist or antagonist of the nuclear receptor. (A, B) Pioglitazone (Pio) is an agonist of PPARγ and T0070907 is an antagonist of PPARγ. (C, D) Dexamethasone (Dexa) is an agonist of GR and mifepristone is an antagonist of GR. The level of adipocytokines was measured by ELISA. Values represent the means ± SD ($n = 3$).

nm. All compounds are >97% pure by RP-HPLC.

4.2. General procedure for the synthesis of chalcone analogs from dehydroacetic acid and aldehydes

To a solution of dehydroacetic acid (0.01 mol, 1.68 g) in chloroform (25 mL) were added appropriate aldehyde (0.01 mol) and piperidine (0.008 mol). The action mixture was stirred under reflux at 80 °C for 5 h–21 h until TLC analysis indicated complete conversion. The precipitate was filtered, washed several times with ethanol and ether. The filtrate was crystallized from an appropriate solvent (chloroform, ethanol, ether) to give the corresponding chalcone compound.

4.2.1. (E)-4-Hydroxy-3-(3-(4-hydroxy-3-methoxyphenyl)acryloyl)-6-methyl-2H-pyran-2-one (1)

Aldehyde: 4-Hydroxy-3-methoxybenzaldehyde, Reaction time: 8 h, Crystallization solvent: Chloroform, $R_f = 0.21$ (Hex: EA = 3:2), Yield: 68%, Yellow powder, m.p: 250–252 °C, ^{1}H NMR (600 MHz, DMSO−d_6) δ 9.95 (s, 1H), 8.02 (d, $J = 15.6$ Hz, 1H), 7.90 (d, $J = 15.6$ Hz, 1H), 7.30–7.21 (m, 2H), 6.87 (d, $J = 8.2$ Hz, 1H), 6.26 (s, 1H), 3.82 (s, 3H), 2.26 (s, 3H); ^{13}C NMR (75 MHz, DMSO−d_6): δ 191.95, 151.18, 148.45, 147.29, 126.33, 124.19, 119.43, 116.53, 113.10, 102.56, 56.11, 20.51; HRMS *m/z* calculated for $C_{16}H_{14}O_6$ $[M + H]^+$: 303.0863, found: 303.0811; >97% purity (as determined by RP-HPLC, method B, t_R = 10.53 min, method G, t_R = 11.56 min).

4.2.2. (E)-3-(3-(3,4-Dihydroxyphenyl)acryloyl)-4-hydroxy-6-methyl-2H-pyran-2-one (2)

Aldehyde: 3,4-Dihydroxybenzaldehyde, Reaction time: 10 h, Crystallization solvent: Ethanol, $R_f = 0.22$ (Hex: EA = 3:2), Yield: 44%, Orange powder, m.p: 256–258 °C, ^{1}H NMR (600 MHz, DMSO−d_6) δ 7.97 (d, $J = 15.6$ Hz, 1H), 7.82 (d, $J = 15.6$ Hz, 1H), 7.18 (d, $J = 2.0$ Hz, 1H), 7.06 (dd, $J = 8.2$, 2.0 Hz, 1H), 6.81 (d, $J = 8.2$ Hz, 1H), 6.25 (s, 1H), 2.25 (s, 3H); ^{13}C NMR (75 MHz, DMSO−d_6): δ 196.59, 188.11, 174.56, 155.29, 152.25, 151.16, 131.13, 129.12, 123.68, 121.24, 119.49, 107.44, 103.90, 25.23; HRMS *m/z* calculated for $C_{15}H_{12}O_6$ $[M + H]^+$: 289.0707, found: 289.0710; >97% purity (as determined by RP-HPLC, method B, t_R = 6.14 min, method G, t_R = 8.63 min).

4.2.3. (E)-3-(3-(3,4-Dimethoxyphenyl)acryloyl)-4-hydroxy-6-methyl-2H-pyran-2-one (3)

Aldehyde: 3,4-Dimethoxybenzaldehyde, Reaction Time: 12 h, Crystallization solvent: Ethanol, $R_f = 0.25$ (Hex: EA = 3:2), Yield: 39%, Orange powder, m.p: 224–226 °C, ^{1}H NMR (600 MHz, $CDCl_3$) δ 8.21 (d, $J = 15.6$ Hz, 1H), 7.96 (d, $J = 15.6$ Hz, 1H), 7.29 (dd, $J = 8.3$, 1.9 Hz, 1H), 7.22 (d, $J = 1.9$ Hz, 1H), 6.90 (d, $J = 8.3$ Hz, 1H), 5.96 (d, $J = 0.6$ Hz, 1H), 3.96 (s, 3H), 3.94 (s, 3H), 2.28 (d, $J = 0.6$ Hz, 3H); ^{13}C NMR (75 MHz, $CDCl_3$): 192.35, 183.35, 168.28, 161.43, 152.10, 149.27, 146.75, 127.83, 124.47, 120.51, 111.01, 110.46, 102.46, 99.29, 56.02, 55.96, 20.61; HRMS *m/z* calculated for $C_{17}H_{16}O_6$ $[M - H]^-$: 315.0874, found: 315.0862; >97% purity (as determined by RP-HPLC, method B, t_R = 18.06 min, method G, t_R = 16.60 min).

4.2.4. (E)-3-Cinnamoyl-4-hydroxy-6-methyl-2H-pyran-2-one (4)

Aldehyde: Benzaldehyde, Reaction time: 12 h, Crystallization solvent: Ethanol, $R_f = 0.24$ (Hex: EA = 3:1), Yield: 45%, Yellow powder, m.p: 132–134 °C, ^{1}H NMR (600 MHz, $CDCl_3$) δ 8.32 (d, $J = 15.7$ Hz, 1H), 7.97 (d, $J = 15.7$ Hz, 1H), 7.72–7.66 (m, 2H), 7.45–7.39 (m, 3H), 5.97 (d, $J = 0.6$ Hz, 1H), 2.28 (d, $J = 0.6$ Hz, 3H); ^{13}C NMR (75 MHz, $CDCl_3$): 192.81, 183.17, 168.66, 161.27, 146.36,134.73, 131.12, 129.20, 128.96, 123.02, 102.42, 99.49, 20.66; HRMS *m/z* calculated for $C_{15}H_{12}O_4$ $[M - H]^-$: 256.0736, found: 256.0731; >97% purity (as determined by RP-HPLC, method A, t_R = 11.67 min, method E, t_R = 9.84 min). Analytical data were the same as previously reported [47].

4.2.5. (E)-3-(3-(3,4-Dimethylphenyl)acryloyl)-4-hydroxy-6-methyl-2H-pyran-2-one (5)

Aldehyde: 3,4-Dimethylbenzaldehyde, Reaction time: 5 h, Crystallization solvent: Ether, $R_f = 0.21$ (Hex: EA = 3:1), Yield: 36%, Yellow powder, m.p: 108–110 °C, ^{1}H NMR (600 MHz, $CDCl_3$) δ 8.25 (d, $J = 15.7$ Hz, 1H), 7.93 (d, $J = 15.7$ Hz, 1H), 7.45 (d, $J = 1.5$ Hz, 1H), 7.42 (dd, $J = 7.8$, 1.5 Hz, 1H), 7.16 (d, $J = 7.8$ Hz, 1H), 5.93 (d, $J = 0.6$ Hz, 1H), 2.29 (s, 6H), 2.26 (d, $J = 0.6$ Hz, 3H); ^{13}C NMR (150 MHz, $CDCl_3$) δ 205.26, 192.67, 183.32, 181.09, 169.10, 168.44, 161.30, 146.94, 140.78, 137.30, 132.43, 130.28, 127.14, 121.57, 102.54, 101.45, 99.37, 30.07, 20.66, 19.98, 19.70; HRMS *m/z* calculated for $C_{17}H_{16}O_4$ $[M + H]^+$: 285.1122, found: 285.1127; >97% purity (as determined by RP-HPLC, method C, t_R = 5.86 min, method H, t_R = 5.32 min). Analytical data were the same as previously reported [47].

4.2.6. (E)-3-(3-(4-Fluoro-3-methoxyphenyl)acryloyl)-4-hydroxy-6-methyl-2H-pyran-2-one (6)

Aldehyde: 4-Fluoro-3-methoxybenzaldehyde, Reaction time: 12 h,

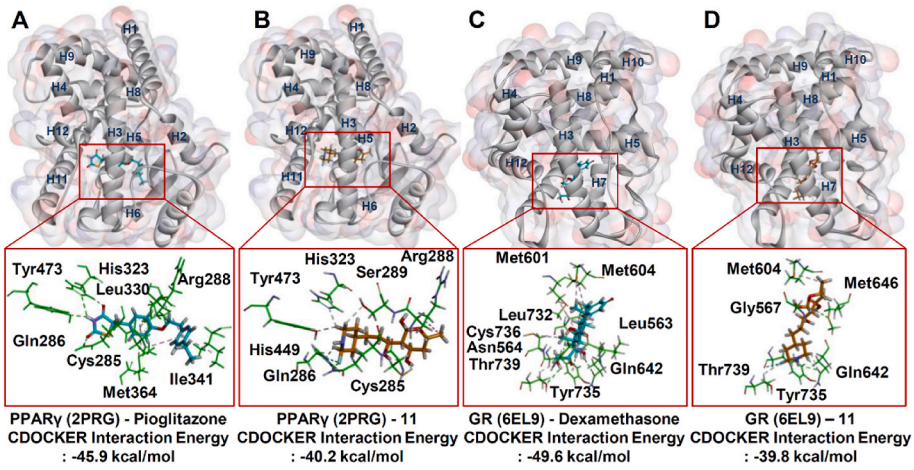

Fig. 5. Molecular docking modes of compound **11** against human PPARγ and GR structures. The ligand-receptor interactions for PPARγ were analyzed with the structure acquired from the RCSB PDB ID 2PRG with the BIOVIA Discovery Studio software. Optimized binding modes of PPARγ with pioglitazone (A) and compound **11** (B). The GR interaction models for dexamethasone (C) and compound **11** (D) were analyzed with RCSB PDB ID 6EL9. Optimized binding modes between ligands and protein structures were visualized using BIOVIA Discovery Studio software.

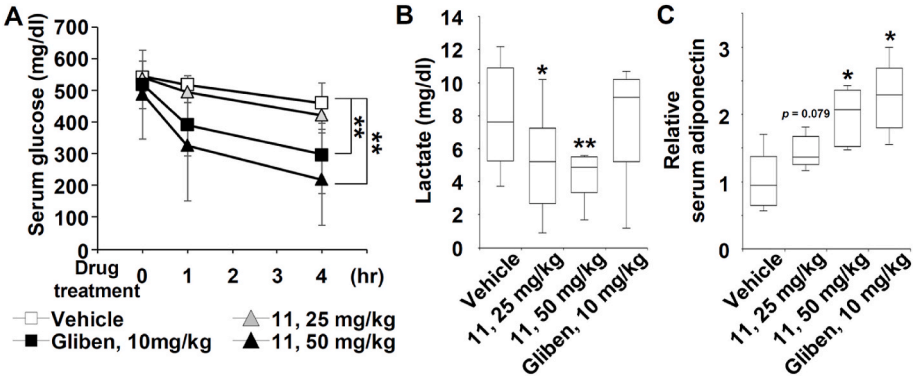

Fig. 6. Effects of compound **11** on STZ-induced diabetic mice. STZ-induced diabetic C57BL/6J mice were orally administered with a vehicle, glibenclamide (Gliben) as a positive anti-diabetic control or compound **11** for 5 days. (A) On the 2nd day of the administration, serum glucose level was measured just before drug treatment (0 h), and at 1 and 4 h after drug treatment ($n = 7$, mean ± SD, $^{**}p \leq 0.01$). (B) Serum lactate level was measured on the 5th day of drug treatment ($n = 7$, mean ± SD, $^{*}p \leq 0.05$, $^{**}p \leq 0.01$). (C) Serum adiponectin level was also quantified on the 5th day of drug treatment ($n = 4$ in the group treated with 25 mg/kg of compound **11**, $n = 7$ in the other groups, mean ± SD, $^{*}p \leq 0.05$).

Crystallization solvent: Ether, $R_f = 0.14$ (Hex: EA = 5:1), Yield: 36%, Yellow powder, m.p: 174–176 °C, ^{1}H NMR (600 MHz, $CDCl_3$) δ 8.23 (d, $J = 15.7$ Hz, 1H), 7.89 (d, $J = 15.7$ Hz, 1H), 7.26–7.23 (m, 2H), 7.16–7.07 (m, 1H), 5.97 (s, 1H), 3.96 (s, 3H), 2.29 (s, 3H); ^{13}C NMR (75 MHz, $CDCl_3$): 192.60, 183.12, 168.74, 161.34, 148.18, 145.33, 131.47, 131.42, 123.11, 123.02, 122.79, 122.76, 116.68, 116.43, 113.03, 113.00, 102.41, 99.44, 56.30, 20.68; HRMS *m/z* calculated for $C_{15}H_{12}FO_5$ $[M + H]^+$: 305.0819, found: 305.0821; >97% purity (as determined by RP-HPLC, method A, $t_R = 12.06$ min, method F, $t_R = 14.43$ min).

4.2.7. (E)-3-(3-(4-Fluorophenyl)acryloyl)-4-hydroxy-6-methyl-2H-pyran-2-one (7)

Aldehyde: 4-Fluorobenzaldehyde, Reaction time: 21 h, Crystallization solvent: Ethanol, $R_f = 0.25$ (Hex: EA = 6:1), Yield: 36%, Ivory powder, m.p: 132–134 °C, ^{1}H NMR (300 MHz, $CDCl_3$): 8.24 (d, $J = 15.6$ Hz, 1H), 7.91 (d, $J = 15.6$ Hz, 1H), 7.70–7.66 (m, 2H), 7.13–7.08 (m, 2H), 5.96 (s, 1H), 2.28 (s, 3H); ^{13}C NMR (75 MHz, $CDCl_3$): δ 192.68, 183.13, 168.75, 161.27, 144.92, 131.23, 131.12, 122.81, 116.33, 116.04, 102.39, 20.67 (CH_3); HRMS *m/z* calculated for $C_{15}H_{11}FO_4$ $[M + H]^+$: 275.0714, found: 275.0830; >97% purity (as determined by RP-HPLC, method A, $t_R = 12.01$ min, method F, $t_R = 14.29$ min). Analytical data were the same as previously reported [47].

4.2.8. (E)-3-(3-(3,4-Difluorophenyl)acryloyl)-4-hydroxy-6-methyl-2H-pyran-2-one (8)

Aldehyde: 3,4-Difluorobenzaldehyde, Reaction time: 15 h, Crystallization solvent: Ethanol, $R_f = 0.17$ (Hex: EA = 5:1), Yield: 45%, Yellow powder, m.p: 176–178 °C, ^{1}H NMR (300 MHz, $CDCl_3$): δ 8.24 (d, $J = 15.8$ Hz, 1H), 7.84 (d, $J = 15.8$ Hz, 1H), 7.56–7.49 (m, 1H), 7.45–7.41 (m, 1H), 7.28–7.18 (m, 1H), 5.99 (s, 1H), 2.32 (s, 3H); ^{13}C NMR (75 MHz, $CDCl_3$); 192.51, 182,98, 169,05, 161.22, 143.49, 132.03, 125.84, 124.15, 117.96, 117.84, 117.36, 117.24, 102.27, 99.51, 20.71; HRMS *m/z* calculated for $C_{15}H_{10}F_2O_4$ $[M + H]^+$: 293.0619, found: 293.0617; >97% purity (as determined by RP-HPLC, method A, $t_R = 13.43$ min, method F, $t_R = 16.52$ min). Analytical data were the same as previously reported [47].

4.2.9. (E)-3-(3-(3,5-Difluorophenyl)acryloyl)-4-hydroxy-6-methyl-2H-pyran-2-one (9)

Aldehyde: 3,5-Difluorobenzaldehyde, Reaction time: 17 h, Crystallization solvent: Ethanol, $R_f = 0.20$ (Hex: EA = 5:1), Yield: 47%, Yellow powder, m.p: 182–184 °C, ^{1}H NMR (300 MHz, DMSO−d_6): 8.11 (d, $J = 15.6$ Hz, 1H), 7.83 (d, $J = 15.9$ Hz, 1H), 7.50–7.48 (m, 2H), 7.39–7.38 (m, 1H), 6.36 (s, 1H), 2.29 (s, 3H); ^{13}C NMR (75 Hz, $CDCl_3$): δ 192.54, 182.88, 169.25, 161.12, 143.01, 142.97, 137.98, 125.78, 111.68, 111.34, 105.98, 102.16, 99.63, 20.73; HRMS *m/z* calculated for $C_{15}H_{10}F_2O_4$ $[M + H]^+$: 293.0619, found: 293.0616; >97% purity (as determined by RP-HPLC, method A, $t_R = 14.08$ min, method E, $t_R = 11.47$ min).

4.2.10. (E)-4-Hydroxy-6-methyl-3-(3-(pyridine-4-yl)acryloyl)-2H-pyran-2-one (10)

Aldehyde: 4-Pyridinecarboxaldehyde, Reaction time: 12 h, Crystallization solvent: Chloroform/Ether, $R_f = 0.26$ (Hex:EA = 2:3), Yield: 50%, Yellow powder, m.p: 158–160 °C, ^{1}H NMR (600 MHz, $CDCl_3$) δ 8.69 (dd, $J = 4.5$, 1.6 Hz, 2H), 8.43 (d, $J = 15.8$ Hz, 1H), 7.80 (d, $J = 15.8$ Hz, 1H), 7.51 (dd, $J = 4.5$, 1.6 Hz, 2H), 6.00 (s, 1H), 2.31 (s, 3H); ^{13}C NMR (75 MHz, $CDCl_3$): 192.60, 182.83, 169.47, 161.10, 150.65, 142.43, 141.82, 127.65, 122.40, 102.11, 99.73, 20.77; HRMS *m/z*

calculated for $C_{14}H_{11}NO_4$ $[M + H]^+$: 258.0760, found: 258.0763; >97% purity (as determined by RP-HPLC, method D, $t_R = 7.89$ min, method I, $t_R = 8.83$ min).

4.2.11. (E)-3-(3-(2-Fluoropyridin-4-yl)acryloyl)-4-hydroxy-6-methyl-2H-pyran-2-one (11)

Aldehyde: 2-Fluoropyridine-4-carboxaldehyde, Reaction time: 7 h, Crystallization solvent: Ether, $R_f = 0.19$ (Hex: EA = 5:2), Yield: 31%, Yellow powder, m.p: 204–206 °C, ^{1}H NMR (600 MHz, $CDCl_3$) δ 8.42 (d, J = 15.8 Hz, 1H), 8.29 (d, J = 5.2 Hz, 1H), 7.77 (d, J = 15.8 Hz, 1H), 7.41 (d, J = 5.2 Hz, 1H), 7.13 (s, 1H), 6.02 (s, 1H), 2.32 (s, 3H); ^{13}C NMR (150 MHz, $CDCl_3$) δ 192.37, 182.70, 169.71, 164.45 (d, J = 238 Hz), 161.04, 148.44, 147.47, 140.57, 128.88, 120.00, 108.52 (d, J = 38 Hz), 102.01, 99.76, 20.77; HRMS m/z calculated for $C_{14}H_{10}FNO_4$ $[M + H]^+$: 276.0666, found: 276.0650; >97% purity (as determined by RP-HPLC, method B, $t_R = 10.76$ min, method G, $t_R = 8.67$ min).

4.2.12. (E)-4-hydroxy-6-methyl-3-(3-(pyridin-2-yl)acryloyl)-2H-pyran-2-one (12)

Aldehyde: 3-Pyridinecarboxaldehyde, Reaction time: 12 h, Crystallization solvent: Chloroform/Ether, $R_f = 0.26$ (Hex: EA = 2:3), Yield: 40%, Brown powder, m.p: 144–146 °C, ^{1}H NMR (600 MHz, $CDCl_3$) δ 8.71 (s, 1H), 8.60 (d, J = 15.6 Hz, 1H), 7.93 (d, J = 15.6 Hz, 1H), 7.74 (dd, J = 7.8, 7.0 Hz, 1H), 7.65 (d, J = 7.8 Hz, 1H), 7.29 (d, J = 7.0 Hz, 1H), 5.98 (s, 1H), 2.29 (s, 3H); ^{13}C NMR (75 MHz, $CDCl_3$): 192.60, 182.83, 169.47, 161.10, 150.65, 142.43, 141.82, 127.65, 122.40, 102.11, 99.73, 20.77; HRMS m/z calculated for $C_{14}H_{11}NO_4$ $[M + H]^+$: 258.0760, found: 258.0763; >97% purity (as determined by RP-HPLC, method D, $t_R = 13.65$ min, method H, $t_R = 11.19$ min).

4.2.13. (E)-3-(3-(1H-Indol-3-yl)acryloyl)-4-hydroxy-6-methyl-2H-pyran-2-one (13)

Aldehyde: 1H-indole-3-carbaldehyde, Reaction time: 17 h, Crystallization solvent: Ethyl acetate, $R_f = 0.22$ (Hex: EA = 7:3), Yield: 65%, Red powder, m.p: 264–266 °C, ^{1}H NMR (300 MHz, DMSO−d_6): 12.23 (s, 1H, NH), 8.29–8.15 (m, 3H), 7.97 (d, J = 3.0 Hz, 1H), 7.54 (d, J = 9.0 Hz, 1H), 7.31–7.28 (m, 2H), 6.13 (s, 1H), 2.22 (s, 3H); ^{13}C NMR (75 MHz, DMSO−d_6): 190.66, 183.63, 161.86, 141.47, 138.42, 136.34, 125.25, 123.71, 122.29, 120.58, 114.23, 113.39, 103.90, 98.99, 20.35; HRMS m/z calculated for $C_{17}H_{13}NO_4$ $[M + H]^+$: 296.0917, found: 296.0901; >97% purity (as determined by RP-HPLC, method B, t_R = 19.32 min, method G, $t_R = 18.55$ min).

4.2.14. (E)-4-Hydroxy-6-methyl-3-(3-(thiophen-3-yl)acryloyl)-2H-pyran-2-one (14)

Aldehyde: Thiophene-3-carbaldehyde, Reaction time: 16 h, Crystallization solvent: Ethanol, $R_f = 0.21$ (Hex: EA = 3:1), Yield: 37%, Orange powder, m.p: 174–176 °C, ^{1}H NMR (300 MHz, $CDCl_3$): 8.12 (d, J = 15.6 Hz, 1H), 7.96 (d, J = 15.6 Hz, 1H), 7.68 (s, 1H), 7.49 (d, J = 5.4 Hz, 1H), 7.37 (d, J = 5.4 Hz, 1H), 5.96 (s, 1H), 2.28 (s, 3H); ^{13}C NMR (75 MHz, $CDCl_3$): δ 192.90, 183.18, 168.51, 161.26, 138.64, 130.53, 127.07, 125.95, 122.64, 102.46, 99.38, 20.64; HRMS m/z calculated for $C_{13}H_{10}O_4S$ $[M + H]^+$: 263.0372, found: 263.0357; >97% purity (as determined by RP-HPLC, method B, $t_R = 21.92$ min, method G, t_R = 16.91 min).

4.2.15. (E)-3-(3-(furan-3-yl)acryloyl)-4-hydroxy-6-methyl-2H-pyran-2-one (15)

Aldehyde: Furan-3-carbaldehyde, Reaction time: 6 h, Crystallization solvent: ethanol; $R_f = 0.21$ (Hex: EA = 3:1), Yield 38%, Orange powder, m.p: 176–178 °C, ^{1}H NMR (300 MHz, $CDCl_3$): 8.02 (d, J = 15.6 Hz, 1H), 7.89 (d, J = 15.6 Hz, 1H), 7.77 (s, 1H), 7.47 (s, 1H), 6.79 (s, 1H), 5.95 (s, 1H), 2.28 (s, 3H); ^{13}C NMR (75 MHz, $CDCl_3$): δ 192.52, 183.21, 168.50, 161.23, 146.35, 144.66, 136.45, 123.66, 122.74, 107.97, 102.44, 99.18, 20.62; HRMS m/z calculated for $C_{13}H_{10}O_5$ $[M + H]^+$: 247.0600, found: 247.0603; >97% purity (as determined by RP-HPLC, method B, t_R = 14.16 min, method G, $t_R = 14.16$ min).

4.2.16. (E)-3-(3-(Benzo[d] [1,3]dioxol-5-yl) acryloyl)-4-hydroxy-6-methyl-2H-pyran-2-one (16)

Aldehyde: Benzo[d] [1,3]dioxole-5-carbaldehyde, Reaction time: 10 h, Crystallization solvent: Ethanol, $R_f = 0.21$ (Hex: EA = 5:1), Yield: 33%, Yellow powder, m.p: 198–200 °C, ^{1}H NMR (600 MHz, $CDCl_3$) δ 8.15 (d, J = 15.6 Hz, 1H), 7.90 (d, J = 15.6 Hz, 1H), 7.23 (d, J = 1.5 Hz, 1H), 7.17 (dd, J = 8.0, 1.5 Hz, 1H), 6.84 (d, J = 8.0 Hz, 1H), 6.04 (s, 2H), 5.95 (s, 1H), 2.28 (s, 3H); ^{13}C NMR (75 MHz, $CDCl_3$): 192.43, 183.32, 168.40, 148.50, 146.42, 129.36, 126.38, 120.85, 108.66, 107.41, 102.57, 101.76, 20.65; HRMS m/z calculated for $C_{16}H_{12}O_6$ $[M + H]^+$: 301.0707, found: 301.0710; >97% purity (as determined by RP-HPLC, method A, $t_R = 10.10$ min, method E, $t_R = 9.91$ min).

4.3. Cell growth and the adipogenic differentiation of hBM-MSCs

The hBM-MSCs were commercially acquired from Lonza (Walkersville, MD, USA) and cultured with the Dulbecco's Modified Eagle's Medium (DMEM, glucose 1 g/L), 1% penicillin-streptomycin (Invitrogen, Carlsbad, CA, USA), 1% Glutamax™ (Invitrogen), and 10% fetal bovine serum (FBS). The adipogenesis-inducing chemical cocktail was prepared by mixing DMEM (glucose 4.5 g/L) with 10 μg/ml of insulin, 0.5 μM of dexamethasone, 0.5 mM 3-isobutyl-1-methylxanthine (IBMX) (IDX), 10% FBS and 1% penicillin-streptomycin. Aspirin, glibenclamide, dexamethasone, pioglitazone, WY-14643, rosiglitazone, mifepristone, IBMX, and insulin were acquired from Sigma-Aldrich (St. Louis, MO, USA). T0070907 was purchased from Tocris Bioscience (Bristol, U.K.). The media were replaced every 3rd day during the adipocyte differentiation.

4.4. Oil red O and hematoxylin staining and quantification

To measure the level of the adipogenesis of hBM-MSCs, Oil red O and hematoxylin staining was performed [48,49]. The cells were rinsed twice with phosphate-buffered saline (PBS) solution and fixed with 10% of neutral buffered formalin (pH 7.4) for 40 min. The fixed cells were washed with 60% of isopropyl alcohol solution and dried completely. The lipid droplets of fixed cells were stained with 0.2% ORO solution for 15 min at room temperatures and rinsed three times with tap water. To evaluate the lipid formation, ORO stained cells were dissolved using 100% isopropanol solution for 10 min at 25 °C and the absorbance was evaluated using a spectrometer at 540 nm. To visualize the nucleus of the fixed cells, a hematoxylin reagent was used for 30 s and washed with tap water three times. The stained cells were photographed using Eclipsed TS100 inverted microscope (Nikon Co., Tokyo, Japan).

4.5. Adipocytokine enzyme-linked immunosorbent assay (ELISA)

For quantifying the adiponectin and leptin levels of hBM-MSCs supernatants, Quantikine™ immunoassay kits (R&D systems, Minneapolis, NM, USA) were used. The quantification of adiponectin and leptin level was evaluated with an instrumental setting as described previously [50–52].

4.6. Nuclear receptor (NR) binding assays and in vitro kinase inhibition assays

Human PPARα, PPARγ, PPARδ, and GR radioligand binding assay was performed as previously described [53–56]. The radioligands 200 nM [^{3}H] WY14643, 5 nM [^{3}H] rosiglitazone, 2.5 nM [^{3}H] L-783483, and 5 nM [^{3}H] dexamethasone were used to identify a series of PPARα, PPARγ, PPARδ, and GR ligands, respectively. The IC_{50} values were calculated by a non-linear, least squares regression analysis using MathIQ™ (ID Business Solutions Ltd., UK) and the Ki values were determined using the equation of Cheng and Prusoff. The kinase

inhibition assay was performed as previously described [57]. γ^{32}P-ATP and histone H1 were co-incubated with human CDK5/p25 and CDK5/p35. When the magnesium ATP mixture was added, the reaction was initiated. After incubation at room temperature for 40 min, the reaction was terminated by adding 3% phosphoric acid solution. 10 μl of the reaction mixture was spotted on the P30 filtermat (PerkinElmer, Richmond, CA, USA) and the membrane was washed three times for 5 min using 75 mM phosphoric acid and once for 5 min using methanol. The filtermat was dried at 27 °C for 1hr and the radioactivity was measured by a liquid scintillation counter (Beckman Coulter, Indianapolis, IN, USA).

4.7. Animal experiments

All animal experiments were performed according to protocols approved and reviewed by the Institutional Animal Care and Use Committee in Sahmyook University in accordance with the Animal Care and Use Guidelines of Sahmyook University. In 5-week-old male C57BL/6J mice, diabetes was induced by a single intraperitoneal injection of 180 mg/kg of STZ. From the 7th day after the STZ administration, plasma glucose level was evaluated daily for 3 consecutive days after 2 h of fasting. The plasma glucose level was determined using a portable glucose meter Accu-Check Active (Boehringer-Mannheim Biochemicals, Indianapolis, IN, USA). STZ-induced diabetic mice were defined as plasma glucose values above 300 mg/dL. To investigate the antidiabetic activity, seven STZ-induced diabetic mice were randomly chosen in each experimental group. 0.5% carboxymethylcellulose (CMC) was used for formulating drugs and control groups were administered vehicle. Before the drug treatment, plasma glucose level was measured again at 2 h after fasting and drug candidates were administered orally. On the fifth day, plasma glucose concentration was evaluated just before drug treatment (0 h) and 1and 4h after drug treatment. The blood samples were acquired through the tail vein with heparinized syringes. Plasma lactate levels were evaluated with a lactate assay kit (MAK064, Sigma-Aldrich) and serum adiponectin and leptin levels were measured with Quantikine™ immunoassay kits (R&D systems, Minneapolis, NM, USA) for a mouse.

4.8. Molecular modeling

The ligand-receptor interaction modeling was performed using Discovery Studio software (Dassault Systèmes, BIODIVA Corporation, San Diego, CA, USA). The docking sites of receptor and ligands were set as a sphere, radius 20 Å at the optimal ligand binding site. The protein crystal structures of PPARγ and GR LBD were acquired from the RCSB PDB (PDB ID: 2PRG, and 6EL9). From the top 10 binding modes of each ligand-receptor interaction, binding modes with the lowest CDOCKER energy for each PPARγ and GR were selected for analysis of interaction modes.

4.9. Statistical analysis

RStudio® for Windows (RStudio Inc., Boston, MA, USA) was used for statistical analysis. The means ± standard deviation (SD) from three independent experiments was used for data presentation. Statistical significance was determined by one-way analysis of variance (ANOVA) and post-hoc tests. The threshold of significance was established at $^{*}P \leq 0.05$ and $^{**}P \leq 0.01$.

Declaration of competing interest

The authors declare that they have no known competing financial interests or personal relationships that could have appeared to influence the work reported in this paper.

Data availability

No data was used for the research described in the article.

Acknowledgements

This work was supported by the National Research Foundation (NRF) of Korea (NRF-2018R1A5A2024425, 2019R1A2C2085749, and 2022M3A9B6017654 to M.N., 2019R1A6A1A03031807 and 2020R1A2C2005919 to Y.B).

Appendix A. Supplementary data

Supplementary data to this article can be found online at https://doi.org/10.1016/j.ejmech.2022.114927.

References

[1] J.H. Stern, J.M. Rutkowski, P.E. Scherer, Adiponectin, leptin, and fatty acids in the maintenance of metabolic homeostasis through adipose tissue crosstalk, Cell Metabol. 23 (2016) 770–784, https://doi.org/10.1016/j.cmet.2016.04.011.
[2] A.Y. Kim, Y.J. Park, X. Pan, K.C. Shin, S.H. Kwak, A.F. Bassas, R.M. Sallam, K. S. Park, A.A. Alfadda, A. Xu, J.B. Kim, Obesity-induced DNA hypermethylation of the adiponectin gene mediates insulin resistance, Nat. Commun. 6 (2015) 1–11, https://doi.org/10.1038/ncomms8585.
[3] H. Münzberg, C.D. Morrison, Structure, production and signaling of leptin, Metabolism 64 (2015) 13–23, https://doi.org/10.1016/j.metabol.2014.09.010.
[4] L.G. Straub, P.E. Scherer, Metabolic messengers: adiponectin, Nat. Metab. 1 (2019) 334–339, https://doi.org/10.1038/s42255-019-0041-z.
[5] C.R. Kahn, G. Wang, K.Y. Lee, Altered adipose tissue and adipocyte function in the pathogenesis of metabolic syndrome, J. Clin. Invest. 129 (2019) 3990–4000, https://doi.org/10.1172/JCI129187.
[6] M. Roden, C. Ludwig, P. Nowotny, B. Schneider, M. Clodi, H. Vierhapper, A. Roden, W. Waldhäusl, Relative hypoleptinemia in patients with type 1 and type 2 diabetes mellitus, Int. J. Obes. 24 (2000) 976–981, https://doi.org/10.1038/sj.ijo.0801266.
[7] C.M. Kusminski, P.E. Bickel, P.E. Scherer, Targeting adipose tissue in the treatment of obesity-associated diabetes, Nat. Rev. Drug Discov. 15 (2016) 639–660, https://doi.org/10.1038/nrd.2016.75.
[8] J. Yu, S. Ahn, H.J. Kim, M. Lee, S. Ahn, J. Kim, S.H. Jin, E. Lee, G. Kim, J. H. Cheong, K.A. Jacobson, L.S. Jeong, M. Noh, Polypharmacology of N^6-(3-Iodobenzyl) adenosine-5′-*N*-methyluronamide (IB-MECA) and related A_3 adenosine receptor ligands: peroxisome proliferator activated receptor (PPAR) γ partial agonist and PPARδ antagonist activity suggests their antidiabetic potential, J. Med. Chem. 60 (2017) 7459–7475, https://doi.org/10.1021/acs.jmedchem.7b00805.
[9] O.S. Kwon, S. Ahn, J.E. Jeon, I.G. Park, T.H. Won, C.J. Sim, H.-G. Park, D.-C. Oh, K.-B. Oh, M. Noh, J. Shin, A.-C. Psammocindoles, Isolation, synthesis, and bioactivity of indole-γ-lactams from the sponge *Psammocinia vermis*, Org. Lett. 23 (2021) 4667–4671, https://doi.org/10.1021/acs.orglett.1c01410.
[10] S. Ahn, C.T. Ma, J.M. Choi, S. An, M. Lee, T.H.V. Le, J.J. Pyo, J. Lee, M.S. Choi, S. W. Kwon, J.H. Park, M. Noh, Adiponectin-secretion-promoting phenylethylchromones from the agarwood of *Aquilaria malaccensis*, J. Nat. Prod. 82 (2019) 259–264, https://doi.org/10.1021/acs.jnatprod.8b00635.
[11] M. Noh, Interleukin-17A increases leptin production in human bone marrow mesenchymal stem cells, Biochem. Pharmacol. 83 (2012) 661–670, https://doi.org/10.1016/j.bcp.2011.12.010.
[12] L. Janderová, M. McNeil, A.N. Murrell, R.L. Mynatt, S.R. Smith, Human mesenchymal stem cells as an in vitro model for human adipogenesis, Obes. Res. 11 (2003) 65–74, https://doi.org/10.1038/oby.2003.11.
[13] S. Haliakon, L. Doaré, F. Foufelle, M. Kergoat, M. Guerre-Millo, M.F. Berthault, I. Dugail, J. Morin, J. Auwerx, P. Ferré, Pioglitazone induces in vivo adipocyte differentiation in the obese Zucker fa/fa rat, Diabetes 46 (1997) 1393–1399, https://doi.org/10.2337/diab.46.9.1393.
[14] M. Li, X. Chi, Y. Wang, S. Setrerrahmane, W. Xie, H. Xu, Trends in insulin resistance: insights into mechanisms and therapeutic strategy, Signal Transduct. Targeted Ther. 7 (2022) 216, https://doi.org/10.1038/s41392-022-01073-0.
[15] B. Gross, M. Pawlak, P. Lefebvre, B. Staels, PPARs in obesity-induced T2DM, dyslipidaemia and NAFLD, Nat. Rev. Endocrinol. 13 (2017) 36–49, https://doi.org/10.1038/nrendo.2016.135.
[16] M.J. Lee, S.K. Fried, The glucocorticoid receptor, not the mineralocorticoid receptor, plays the dominant role in adipogenesis and adipokine production in human adipocytes, Int. J. Obes. 38 (2014) 1228–1233, https://doi.org/10.1038/ijo.2014.6.
[17] D. van der Poorten, C.F. Samer, M. Ramezani-Moghadam, S. Coulter, M. Kacevska, D. Schrijnders, L.E. Wu, D. McLeod, E. Bugianesi, M. Komuta, T. Roskams, C. Liddle, L. Hebbard, J. George, Hepatic fat loss in advanced nonalcoholic steatohepatitis: are alterations in serum adiponectin the cause? Hepatology 57 (2013) 2180–2188, https://doi.org/10.1002/hep.26072.
[18] J.H. Choi, A.S. Banks, J.L. Estall, S. Kajimura, P. Boström, D. Laznik, J.L. Ruas, M. J. Chalmers, T.M. Kamenecka, M. Blüher, P.R. Griffin, B.M. Spiegelman, Anti-diabetic drugs inhibit obesity-linked phosphorylation of PPARγ by Cdk5, Nature 466 (2010) 451–456, https://doi.org/10.1038/nature09291.

[19] J.H. Choi, A.S. Banks, T.M. Kamenecka, S.A. Busby, M.J. Chalmers, N. Kumar, D. S. Kuruvilla, Y. Shin, Y. He, J.B. Bruning, D.P. Marciano, M.D. Cameron, D. Laznik, M.J. Jurczak, S.C. Schürer, D. Vidović, G.I. Shulman, B.M. Spiegelman, P.R. Griffin, Antidiabetic actions of a non-agonist PPARγ ligand blocking Cdk5-mediated phosphorylation, Nature 477 (2011) 477–481, https://doi.org/10.1038/nature10383.

[20] R.T. Nolte, G.B. Wisely, S. Westin, J.E. Cobb, M.H. Lambert, R. Kurokawa, M. G. Rosenfeld, T.M. Willson, C.K. Glass, M.V. Milburn, Ligand binding and co-activator assembly of the peroxisome proliferator-activated receptor-γ, Nature 395 (1998) 137, https://doi.org/10.1038/25931.

[21] S. Sauer, Ligands for the nuclear peroxisome proliferator-activated receptor gamma, Trends Pharmacol. Sci. 36 (2015) 688–704, https://doi.org/10.1016/j.tips.2015.06.010.

[22] L. Ripa, K. Edman, M. Dearman, G. Edenro, R. Hendrickx, V. Ullah, H.F. Chang, M. Lepistö, D. Chapman, S. Geschwindner, L. Wissler, P. Svanberg, K. Lawitz, J. Malmberg, A. Nikitidis, R.I. Olsson, J. Bird, A. Llinas, T. Hegelund-Myrbäck, M. Berger, P. Thorne, R. Harrison, C. Köhler, T. Drmota, Discovery of a novel oral glucocorticoid receptor modulator (AZD9567) with improved side effect profile, J. Med. Chem. 61 (2018) 1785–1799.

[23] R.K. Bledsoe, V.G. Montana, T.B. Stanley, C.J. Delves, C.J. Apolito, D.D. McKee, T. G. Consler, D.J. Parks, E.L. Stewart, T.M. Willson, M.H. Lambert, J.T. Moore, K. H. Pearce, H.E. Xu, Crystal structure of the glucocorticoid receptor ligand binding domain reveals a novel mode of receptor dimerization and coactivator recognition, Cell 110 (2002) 93–105, https://doi.org/10.1016/S0092-8674(02)00817-6.

[24] D.E. Hurt, S. Suzuki, T. Mayama, E. Charmandari, T. Kino, Structural analysis on the pathologic mutant glucocorticoid receptor ligand-binding domains, Mol. Endocrinol. 30 (2016) 173–188, https://doi.org/10.1210/me.2015-1177.

[25] E.R. Weikum, M.T. Knuesel, E.A. Ortlund, K.R. Yamamoto, Glucocorticoid receptor control of transcription: precision and plasticity via allostery, Nat. Rev. Mol. Cell Biol. 18 (2017) 159–174, https://doi.org/10.1038/nrm.2016.152.

[26] B. Kauppi, C. Jakob, M. Färnegårdh, J. Yang, H. Ahola, M. Alarcon, K. Calles, O. Engström, J. Harlan, S. Muchmore, A.K. Ramqvist, S. Thorell, L. Öhman, J. Greer, J.A. Gustafsson, J. Carlstedt-Duke, M. Carlquist, The three-dimensional structures of antagonistic and agonistic forms of the glucocorticoid receptor ligand-binding domain: RU-486 induces a transconformation that leads to active antagonism, J. Biol. Chem. 278 (2003) 22748–22754, https://doi.org/10.1074/jbc.M212711200.

[27] D.W. Ray, C.S. Suen, A. Brass, J. Soden, A. White, Structure/function of the human glucocorticoid receptor: tyrosine 735 is important for transactivation, Mol. Endocrinol. 13 (1999) 1855–1863, https://doi.org/10.1210/mend.13.11.0376.

[28] U. Lind, P. Greenidge, M. Gillner, K.F. Koehler, A. Wright, J. Carlstedt-Duke, Functional probing of the human glucocorticoid receptor steroid-interacting surface by site-directed mutagenesis: Gln-642 plays an important role in steroid recognition and binding, J. Biol. Chem. 275 (2000) 19041–19049, https://doi.org/10.1074/jbc.M000228200.

[29] M. Waragai, G. Ho, Y. Takamatsu, Y. Shimizu, H. Sugino, S. Sugama, T. Takenouchi, E. Masliah, M. Hashimoto, Dual-therapy strategy for modification of adiponectin receptor signaling in aging-associated chronic diseases, Drug Discov 23 (2018) 1305–1311, https://doi.org/10.1016/j.drudis.2018.05.009.

[30] M.A. Tsoukas, O.M. Farr, C.S. Mantzoros, Leptin in congenital and HIV-associated lipodystrophy, Metabolism 64 (2015) 47–59, https://doi.org/10.1016/j.metabol.2014.07.017.

[31] Y. Wu, Y. Dong, M. Atefi, Y. Liu, Y. Elshimali, J.V. Vadgama, Lactate, a neglected factor for diabetes and cancer interaction, Mediat. Inflamm. (2016) 1–12, https://doi.org/10.1155/2016/6456018, 2016.

[32] T. Yamauchi, T. Kadowaki, Adiponectin receptor as a key player in healthy longevity and obesity-related diseases, Cell Metabol. 17 (2013) 185–196, https://doi.org/10.1016/j.cmet.2013.01.001.

[33] H.C. Denroche, J. Levi, R.D. Wideman, R.M. Sequeira, F.K. Huynh, S.D. Covey, T. J. Kieffer, Leptin therapy reverses hyperglycemia in mice with streptozotocin-induced diabetes, independent of hepatic leptin signaling, Diabetes 60 (2011) 1414–1423, https://doi.org/10.2337/db10-0958.

[34] R. Coppari, C. Bjørbæk, Leptin revisited: its mechanism of action and potential for treating diabetes, Nat. Rev. Drug Discov. 11 (2012) 692–708, https://doi.org/10.1038/nrd3757.

[35] A.U. Hasan, K. Ohmori, T. Hashimoto, K. Kamitori, F. Yamaguchi, A. Rahman, M. Tokuda, H. Kobori, PPARγ activation mitigates glucocorticoid receptor-induced excessive lipolysis in adipocytes via homeostatic crosstalk, J. Cell. Biochem. 119 (2018) 4627–4635, https://doi.org/10.1002/jcb.26631.

[36] S.J. Desmet, K. De Bosscher, Glucocorticoid receptors: finding the middle ground, J. Clin. Invest. 127 (2017) 1136–1145, https://doi.org/10.1172/JCI88886.

[37] J. Vandewalle, A. Luypaert, K. De Bosscher, C. Libert, Therapeutic mechanisms of glucocorticoids, Trends Endocrinol. Metabol. 29 (2018) 42–54, https://doi.org/10.1016/j.tem.2017.10.010.

[38] J. Deckers, N. Bougarne, V. Mylka, S. Desmet, A. Luypaert, M. Devos, G. Tanghe, J. V. Moorleghem, M. Vanheerswynghels, L.D. Cauwer, J. Thommis, M. Vuylsteke, J. Tavernier, B.N. Lambrecht, H. Hammad, K. De Bosscher, Co-activation of glucocorticoid receptor and peroxisome proliferator–activated receptor-γ in murine skin prevents worsening of atopic march, J. Invest. Dermatol. 138 (2018) 1360–1370, https://doi.org/10.1016/j.jid.2017.12.023.

[39] S. Lahiri, T. Sen, G. Palit, Involvement of glucocorticoid receptor and peroxisome proliferator activated receptor-γ in pioglitazone mediated chronic gastric ulcer healing in rats, Eur. J. Pharmacol. 609 (2009) 118–125, https://doi.org/10.1016/j.ejphar.2009.03.005.

[40] M. Demerjian, E.H. Choi, M.Q. Man, S. Chang, P.M. Elias, K.R. Feingold, Activators of PPARs and LXR decrease the adverse effects of exogenous glucocorticoids on the epidermis, Exp. Dermatol. 18 (2009) 643–649, https://doi.org/10.1111/j.1600-0625.2009.00841.x.

[41] S. Agrawal, M.A. Chanley, D. Westbrook, X. Nie, T. Kitao, A.J. Guess, R. Benndorf, G. Hidalgo, W.E. Smoyer, Pioglitazone enhances the beneficial effects of glucocorticoids in experimental nephrotic syndrome, Sci. Rep. 6 (2016) 1–9, https://doi.org/10.1038/srep24392.

[42] A.A. Tahrani, A.H. Barnett, C.J. Bailey, Pharmacology and therapeutic implications of current drugs for type 2 diabetes mellitus, Nat. Rev. Endocrinol. 12 (2016) 566–592, https://doi.org/10.1038/nrendo.2016.86.

[43] S. Sblano, C. Cerchia, A. Laghezza, L. Piemontese, L. Brunetti, R. Leuci, F. Gilardi, A. Thomas, M. Genovese, A. Santi, P. Tortorella, P. Paoli, A. Lavecchia, F. Loiodice, A chemoinformatics search for peroxisome proliferator-activated receptors ligands revealed a new pan-agonist able to reduce lipid accumulation and improve insulin sensitivity, Eur. J. Med. Chem. 235 (2022), 114240, https://doi.org/10.1016/j.ejmech.2022.114240.

[44] Y. Yang, Y. Zhao, W. Li, Y. Wu, X. Wang, Y. Wang, T. Liu, T. Ye, Y. Xie, Z. Cheng, J. He, P. Bai, Y. Zhang, L. Ouyang, Emerging targets and potential therapeutic agents in non-alcoholic fatty liver disease treatment, Eur. J. Med. Chem. 197 (2020), 112311, https://doi.org/10.1016/j.ejmech.2020.112311.

[45] S. Chigurupati, S.A. Dhanaraj, P. Balakumar, A step ahead of PPARγ full agonists to PPARγ partial agonists: therapeutic perspectives in the management of diabetic insulin resistance, Eur. J. Pharmacol. 755 (2015) 50–57, https://doi.org/10.1016/j.ejphar.2015.02.043.

[46] K. Liu, X. Zhao, X. Qi, D.-L. Hou, H.-B. Li, Y.-H. Gu, Q.-L. Xu, Design, synthesis, and biological evaluation of a novel dual peroxisome proliferator-activated receptor alpha/delta agonist for the treatment of diabetic kidney disease through anti-inflammatory mechanisms, Eur. J. Med. Chem. 218 (2021), 113388, https://doi.org/10.1016/j.ejmech.2021.113388.

[47] M.Y. Xi, Z.Y. Sun, H.P. Sun, J.M. Jia, Z.Y. Jiang, L. Tao, M. Ye, X. Yang, Y.J. Wang, X. Xue, J.J. Huang, Y. Gao, X.K. Guo, S.L. Zhang, Y.R. Yang, Q.L. Guo, R. Hu, Q. D. You, Synthesis and bioevaluation of a series of α-pyrone derivatives as potent activators of Nrf2/ARE pathway (part I), Eur. J. Med. Chem. 66 (2013) 364–371, https://doi.org/10.1016/j.ejmech.2013.06.007.

[48] S. Ahn, S. An, M. Lee, E. Lee, J.J. Pyo, J.H. Kim, M.W. Ki, S.H. Jin, J. Ha, M. Noh, A long-wave UVA filter avobenzone induces obesogenic phenotypes in normal human epidermal keratinocytes and mesenchymal stem cells, Arch. Toxicol. 93 (2019) 1903–1915, https://doi.org/10.1007/s00204-019-02462-1.

[49] S. Ahn, J. Kim, S. An, J.J. Pyo, D. Jung, J. Lee, S.Y. Hwang, J. Gong, I. Shin, H. P. Kim, H. Kim, M. Noh, 2-Phenyl-8-(1-phenylallyl)-chromenone compounds have a pan-PPAR modulator pharmacophore, Bioorg. Med. Chem. 27 (2019) 2948–2958, https://doi.org/10.1016/j.bmc.2019.05.028.

[50] Y. Han, J. Liu, S. Ahn, S. An, H. Ko, J.C. Shin, S.H. Jin, M.W. Ki, S.H. Lee, K.H. Lee, S.S. Shin, W.J. Choi, M. Noh, Diallyl biphenyl-type neolignans have a pharmacophore of PPARα/γ dual modulators, Biomol. Ther. 28 (2020) 397, https://doi.org/10.4062/biomolther.2019.180.

[51] S. Ahn, M. Lee, S. An, S. Hyun, J. Hwang, J. Lee, M. Noh, 2-Formyl-komarovicine promotes adiponectin production in human mesenchymal stem cells through PPARγ partial agonism, Bioorg. Med. Chem. 26 (2018) 1069–1075, https://doi.org/10.1016/j.bmc.2018.01.019.

[52] J.K. Lee, H.E. Lee, G. Yang, K.B. Kim, S.J. Kwack, J.Y. Lee, *Para*-phenylenediamine, an oxidative hair dye ingredient, increases thymic stromal lymphopoietin and proinflammatory cytokines causing acute dermatitis, Toxicol. Res. 36 (2020) 329–336, https://doi.org/10.1007/s43188-020-00041-6.

[53] R. Seethala, R. Golla, Z. Ma, H. Zhang, K. O'Malley, J. Lippy, L. Cheng, K. Mookhtiar, D. Farrelly, L. Zhang, N. Hariharan, P.T.W. Cheng, A rapid, homogeneous, fluorescence polarization binding assay for peroxisome proliferator-activated receptors alpha and gamma using a fluorescein-tagged dual PPARα/γ activator, Anal. Biochem. 363 (2007) 263–274, https://doi.org/10.1016/j.ab.2007.01.022.

[54] S. Ahn, M.B. Gowda, M. Lee, J.N. Masagalli, K. Mailar, W.J. Choi, M. Noh, Novel linked butanolide dimer compounds increase adiponectin production during adipogenesis in human mesenchymal stem cells through peroxisome proliferator-activated receptor γ modulation, Eur. J. Med. Chem. 187 (2020), 111969, https://doi.org/10.1016/j.ejmech.2019.111969.

[55] J. Berger, M.D. Leibowitz, T.W. Doebber, A. Elbrecht, B. Zhang, G. Zhou, C. Biswas, C.A. Cullinan, N.S. Hayes, Y. Li, M. Tanen, J. Ventre, M.S. Wu, G.D. Berger, R. Mosley, R. Marquis, C. Santini, S.P. Sahoo, R.L. Tolman, R.G. Smith, D.E. Moller, Novel peroxisome proliferator-activated receptor (PPAR) γ and PPARδ ligands produce distinct biological effects, J. Biol. Chem. 274 (1999) 6718–6725, https://doi.org/10.1074/jbc.274.10.6718.

[56] C. Honer, K. Nam, C. Fink, P. Marshall, G. Ksander, R.E. Chatelain, W. Cornell, R. Steele, R. Schweitzer, C. Schumacher, Glucocorticoid receptor antagonism by cyproterone acetate and RU486, Mol. Pharmacol. 63 (2003) 1012–1020, https://doi.org/10.1124/mol.63.5.1012.

[57] S. Ahn, D.M. Jang, S.C. Park, S. An, J. Shin, B.W. Han, M. Noh, Cyclin-dependent kinase 5 inhibitor butyrolactone I elicits a partial agonist activity of peroxisome proliferator-activated receptor γ, Biomolecules 10 (2020) 275, https://doi.org/10.3390/biom10020275.